

*Title:*

# EXPERIMENTAL STUDY OF INDEPENDENT AND CUMULATIVE PRODUCT YIELDS IN $^{208}$ , $^{207}$ , $^{206}$ , $^{nat}$ PB AND $^{209}$ BI TARGETS IRRADIATED WITH 0.04-2.6 GEV PROTONS

*Author(s):*

Yu. E. Titarenko, V. F. Batyaev, V. M. Zhivun, R. D. Mulambetov, S. V. Mulambetova, S. L. Zaitsev, K. A. Lipatov, S. G. Mashnik <sup>1</sup>

Institute for Theoretical and Experimental Physics  
(ITEP), B.Cheremushkinskaya 25, 117259 Moscow,  
Russia

<sup>1</sup> Los Alamos National Laboratory, Los Alamos, NM  
87545, USA

*Submitted to:*

Proc. of the Seventh Meeting on Shielding Aspects of  
Accelerators, Targets and Irradiation Facilities (SATIF-7), Instituto  
Technologico e Nuclear (ITN) Sacavem (Lisbon) Portugal, May  
17-18, 2004

<http://lib-www.lanl.gov/cgi-bin/getfile?00783500.pdf>

# EXPERIMENTAL STUDY OF INDEPENDENT AND CUMULATIVE PRODUCT YIELDS IN $^{208, 207, 206, \text{nat}}\text{Pb}$ AND $^{209}\text{Bi}$ TARGETS IRRADIATED WITH 0.04-2.6 GEV PROTONS

Yu. E. Titarenko, V. F. Batyaev, V. M. Zhivun, R. D. Mulambetov, S. V. Mulambetova, S. L. Zaitsev,  
K. A. Lipatov, S. G. Mashnik<sup>1</sup>

Institute for Theoretical and Experimental Physics (ITEP),

B.Cheremushkinskaya 25, 117259 Moscow, Russia

<sup>1</sup> Los Alamos National Laboratory, Los Alamos, NM 87545, USA

## Abstract.

More than 5000 independent and cumulative yields of radioactive residual product nuclides with life-times ranging from 13.2 min ( $^{187}\text{Re}$ ) to 31.55 years ( $^{207}\text{Bi}$ ) are measured in the  $^{208, 207, 206, \text{nat}}\text{Pb}$  and  $^{209}\text{Bi}$  thin targets irradiated by 0.04, 0.07, 0.10, 0.15, 0.25, 0.40, 0.60, 0.80, 1.20, 1.60, and 2.60 GeV external proton beams from the ITEP U10 accelerator. The  $^{27}\text{Al}(\text{p},\text{x})^{22}\text{Na}$  reaction was used as monitor. The experiments were made using the direct gamma-spectrometry method based on a Ge detector with a 1.8 keV resolution at a 1332 keV  $^{60}\text{Co}$  gamma-line. The measured gamma-spectra were processed by the GENIE2000 code. The residual product nuclides were identified, and their independent and cumulative yields determined, using the PCNUDAT database and the ITEP-designed SIGMA code.

## Introduction

The cross sections/yields of residual product nuclei are of great importance when estimating such basic radiation-technology characteristics of ADS hybrid facility targets as the total target activity, target "poisoning", buildup of long-lived nuclides, product nuclide (Po) alpha-activity, content of low-pressure evaporated nuclides (Hg), evolution of gaseous reaction products, production of chemically-active nuclides that spoil drastically the corrosion resistance of the facility structure materials, etc.

The present-day insufficient accuracy or even absence of needed cross sections has supported a set of experiments to measure the independent and cumulative yields of radioactive residual product nuclides in thin Pb and Bi samples under 0.04-2.60 GeV proton irradiation [1].

## Experiment

The experimental techniques are described in detail in [2-4]. The actual experiments were made using monoisotopic target samples of the following composition:  $^{208}\text{Pb}$ ( $^{206}\text{Pb}$ =0.87%,  $^{207}\text{Pb}$ =1.93%,  $^{208}\text{Pb}$ =97.2%);  $^{207}\text{Pb}$ ( $^{204}\text{Pb}$ =0.03%,  $^{206}\text{Pb}$ =2.61%,  $^{207}\text{Pb}$ =88.3%,  $^{208}\text{Pb}$ =9.06%);  $^{206}\text{Pb}$ ( $^{206}\text{Pb}$ =94.0%,  $^{207}\text{Pb}$ =4.04%,  $^{208}\text{Pb}$ =1.96%);  $^{209}\text{Bi}$ ( $^{204}\text{Pb}$ =1.4%,  $^{206}\text{Pb}$ =24.1%,  $^{207}\text{Pb}$ =22.1%,  $^{208}\text{Pb}$ =52.4%);  $^{209}\text{Bi}$ >99.9%.

The thin  $^{208, 207, 206, \text{nat}}\text{Pb}$  and  $^{209}\text{Bi}$  targets of 10.5 mm diameter (127 - 358 mg/cm<sup>2</sup> thickness) together with aluminum monitors of the same diameter (127 - 254 mg/cm<sup>2</sup> thickness) were irradiated using external beam of ITEP U10 proton synchrotron. The  $^{27}\text{Al}(\text{p},\text{x})^{22}\text{Na}$  reaction was used as monitor. The proton fluencies were from  $3.1 \cdot 10^{13}$  to  $1.4 \cdot 10^{14}$  p/cm<sup>2</sup>. The produced radionuclides were detected using the direct gamma-spectrometry method based on a Ge detector with a 1.8 keV resolution at a

1332 keV  $^{60}\text{Co}$  gamma-line. 40 to 900 mm distances between the irradiated target and the Ge detector cryostat were used to avoid the spectrometer overload. The height dependent efficiency of the spectrometer was obtained using analytical expressions of 100 to 2600 keV absolute efficiencies determined via measurements of the standard gamma-sources. The found efficiencies allowed us to obtain height factors that were used to normalize all the measured gamma-lines intensities to the 40 mm bias height.

Each of the irradiated targets was measured during 3 to 6 months. The gamma spectra were processed via an interactive mode of the GENIE200 program using preliminary results of an automatic mode processing. As an example, Fig. 1 shows measured gamma-spectra from two  $^{nat}\text{Pb}$  targets irradiated with 2.6 GeV (upper) and 0.04 GeV (lower) protons. Both spectra were measured at the same cooling times ( $\sim 6$  days) after the irradiations. The windows demonstrate examples of multiplets resolving.

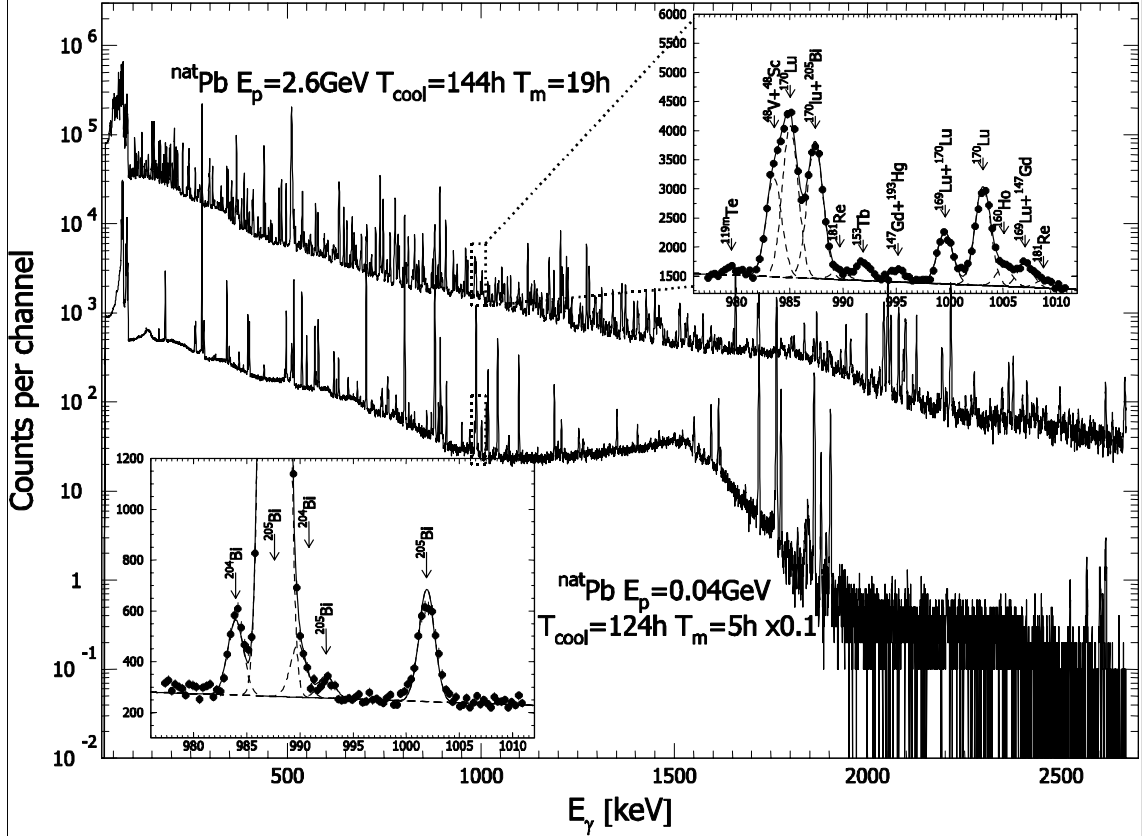


Fig. 1. Gamma-spectra from  $^{nat}\text{Pb}$  targets irradiated with 2.6 GeV (upper figure) and 0.04 GeV (lower figure). The spectra were measured at the same cooling times (140 hours) after the irradiations. The lower spectra was multiplied by 0.1 for visual convenience.

The results of processing of all gamma-spectra of a particular irradiation are compiled into one file which is the input to the SIGMA code. The SIGMA code identifies the measured gamma-lines using the PCNUDAT nuclear decay data base and determines the yields (cross sections) of the produced radionuclides using formulas (1) – (9) derived from the three-chains decay scheme (Fig. 2).

In total, 55 experiments have been conducted. The statistics of the measured products is presented in Table 1. The errors of the measured data are from 10 to 40%. The main contribution to experimental error comes from uncertainty of the monitor reaction cross section, however there are some cases

when the errors are dominated by uncertainties of nuclear data and spectra statistics. The data themselves and their graphical interpretation will be presented in the final technical report of the ISTC Project #2002 and will be uploaded into the EXFOR data base.

### Comparison with data obtained elsewhere

The obtained data are compared with data obtained at other laboratories [5-11]. Most of the data that can be compared with our measurements are from [5] and [11]. Other works provide a minority of such data:  $^{48}\text{V}$ ,  $^{48}\text{Sc}$ ,  $^{46}\text{Sc}$  at 1, 2 and 3 GeV from [6];  $^{83}\text{Rb}$ ,  $^{84}\text{Rb}$ ,  $^{86}\text{Rb}$ ,  $^{106m}\text{Ag}$ ,  $^{110m}\text{Ag}$ ,  $^{110}\text{In}$  and  $^{129}\text{Cs}$  at 0.6 GeV from [7],  $^7\text{Be}$  and  $^{24}\text{Na}$  from [8],  $^7\text{Be}$  at 0.4 GeV from [9];  $^{111}\text{In}$  at 0.45 GeV from [10].

Note that only the work [5] uses the same method as ours, direct kinematics and gamma-spectrometry, allowing a direct comparison of the results. The work [11] uses the inverse kinematics method and its data need to be recalculated to obtain the required cumulative cross sections using the decay branch factors [12]. Figs. 3-6 present several examples from our comparison.

Preliminary comparison of 105 excitation functions from  $^{nat}\text{Pb}$  measured at ITEP with other results obtained via direct kinematics show a satisfactory agreement of most (>90%) of the data. 9 products show deviations above experimental errors ( $^{198}\text{Tl}(\text{c})$ ,  $^{170}\text{Hf}(\text{c})$ ,  $^{173}\text{Lu}(\text{c})$ ,  $^{155}\text{Dy}(\text{c}^*)$ ,  $^{153}\text{Tb}(\text{c}^*)$ ,  $^{145}\text{Eu}(\text{c})$ ,  $^{131}\text{Ba}(\text{c})$ ,  $^{102}\text{Rh}(\text{i})$ ,  $^{101m}\text{Rh}(\text{c})$ , 8 products show deviations above experimental errors at 2.6 GeV ( $^{193m}\text{Hg}(\text{i})$ ,  $^{194(m1+m2+g)}\text{Au}(\text{i})$ ,  $^{183}\text{Re}(\text{c})$ ,  $^{181}\text{Re}(\text{c})$ ,  $^{178}\text{W}(\text{c})$ ,  $^{166}\text{Er}(\text{c})$ ,  $^{160}\text{Er}(\text{c})$ ,  $^{111}\text{In}(\text{c})$ ), 2 products show deviations above experimental errors at 1.6 and 2.6 GeV ( $^{195}\text{Au}(\text{c})$ ,  $^{88(m+g)}\text{Y}(\text{i})$ ), and 4 products deviate above 0.6 GeV energy ( $^{206}\text{Bi}(\text{i})$ ,  $^{205}\text{Bi}(\text{i})$ ,  $^{121}\text{Te}(\text{c})$ ,  $^{114m1}\text{In}(\text{i(m)})$ ). The cause of such discrepancies concerns the methods of processing gamma-spectra and gamma-lines identification, as well as the used databases and monitor reaction cross sections.

Despite of some deviations between the data of ITEP and ZSR [5], these measurements can be used together to produce files of evaluated excitation functions. The data that deviate strongly from each other should be reviewed and, if needed, remeasured.

Our comparison between the ITEP measurements and the GSI data obtained via inverse kinematics data at 0.5 and 1.0 GeV\*A appoints on some systematical discrepancies or/and errors. The mention recalculation of the GSI independent cross section to produce the required cumulative cross sections does not affect the shape of excitation functions but may affect their normalization. Our comparison of the GSI data for 143 products with respective ITEP data shows a good agreement in 119 cases (83%). 24 cases presents discrepancies above experimental errors ( $^{207}\text{Bi}(\text{i})$ ,  $^{199}\text{Pb}(\text{c}^*)$ ,  $^{200}\text{Tl}(\text{i})$ ,  $^{191(m+g)}\text{Au}(\text{i})$ ,  $^{192(m1+g)}\text{Ir}(\text{i})$ ,  $^{190(m+g)}\text{Ir}(\text{i})$ ,  $^{188}\text{Ir}(\text{i})$ ,  $^{186}\text{Ir}(\text{c})$ ,  $^{181}\text{Os}(\text{c})$ ,  $^{172}\text{Ta}(\text{c}^*)$ ,  $^{170}\text{Hf}(\text{c})$ ,  $^{161}\text{Er}(\text{c})$ ,  $^{121}\text{Te}(\text{c})$ ,  $^{105}\text{Rh}(\text{c})$ ,  $^{102}\text{Rh}(\text{i})$ ,  $^{103}\text{Ru}(\text{c})$ ,  $^{99}\text{Mo}(\text{c})$ ,  $^{95}\text{Nb}(\text{c})$ ,  $^{95}\text{Zr}(\text{c})$ ,  $^{86(m+g)}\text{Rb}(\text{i})$ ,  $^{83}\text{Rb}(\text{c})$ ,  $^{82(m+g)}\text{Br}(\text{i})$ ,  $^{72}\text{Ga}(\text{c})$ ,  $^{72}\text{Zn}(\text{c})$ ). Details on the direct and inverse kinematics results comparison is presented in our previous work [14]. The cause of some observed discrepancies concerns uncertainties of the decay chain branching factors as well as monitor reaction cross sections.

Our analysis of the excitation functions measured by different groups shows that the data obtained by similar methods agree better than the data obtained by different methods. The cause of the found discrepancies will be studied further.

A comparison of ITEP data on  $^{209}\text{Bi}$  with respective data from other laboratories is in progress and will be presented in our further works.

Table 1. Total statistics of the measured products from  $^{208, 207, 206}$  Nat Pb and  $^{209}$  Bi.

| Energy (GeV) | Yield type       | $^{Nat}$ Pb | $^{208}$ Pb | $^{207}$ Pb | $^{206}$ Pb | $^{209}$ Bi | Total |
|--------------|------------------|-------------|-------------|-------------|-------------|-------------|-------|
| 2.6          | i                | 16          | 15          | 14          | 14          | 13          | 72    |
|              | $i_{\Sigma m}$   | 16          | 16          | 16          | 16          | 20          | 84    |
|              | $i_{\Sigma m+g}$ | 16          | 14          | 14          | 14          | 13          | 71    |
|              | $c, c^*$         | 123         | 120         | 120         | 120         | 133         | 616   |
| 1.6          | i                | 17          | 17          | 15          | 15          | 13          | 77    |
|              | $i_{\Sigma m}$   | 16          | 17          | 17          | 17          | 18          | 85    |
|              | $i_{\Sigma m+g}$ | 15          | 15          | 15          | 15          | 13          | 73    |
|              | $c, c^*$         | 121         | 123         | 123         | 123         | 127         | 617   |
| 1.2          | i                | 17          | 16          | 16          | 16          | -           | 65    |
|              | $i_{\Sigma m}$   | 16          | 16          | 16          | 16          | -           | 64    |
|              | $i_{\Sigma m+g}$ | 13          | 13          | 13          | 13          | -           | 52    |
|              | $c, c^*$         | 116         | 116         | 116         | 116         | -           | 464   |
| 0.8          | i                | 16          | 16          | 15          | 15          | 14          | 76    |
|              | $i_{\Sigma m}$   | 18          | 19          | 18          | 19          | 21          | 95    |
|              | $i_{\Sigma m+g}$ | 12          | 12          | 12          | 13          | 12          | 61    |
|              | $c, c^*$         | 100         | 99          | 100         | 101         | 100         | 500   |
| 0.6          | i                | 15          | 14          | 14          | 14          | -           | 57    |
|              | $i_{\Sigma m}$   | 18          | 18          | 18          | 18          | -           | 72    |
|              | $i_{\Sigma m+g}$ | 12          | 12          | 12          | 12          | -           | 48    |
|              | $c, c^*$         | 85          | 86          | 85          | 84          | -           | 340   |
| 0.4          | i                | 13          | 13          | 13          | 12          | -           | 51    |
|              | $i_{\Sigma m}$   | 17          | 17          | 16          | 17          | -           | 67    |
|              | $i_{\Sigma m+g}$ | 13          | 13          | 12          | 12          | -           | 50    |
|              | $c, c^*$         | 69          | 66          | 67          | 67          | -           | 269   |
| 0.25         | i                | 13          | 13          | 13          | 12          | -           | 51    |
|              | $i_{\Sigma m}$   | 14          | 14          | 14          | 14          | -           | 56    |
|              | $i_{\Sigma m+g}$ | 9           | 9           | 9           | 9           | -           | 36    |
|              | $c, c^*$         | 52          | 51          | 51          | 52          | -           | 206   |
| 0.15         | i                | 10          | 10          | 11          | 10          | -           | 41    |
|              | $i_{\Sigma m}$   | 12          | 12          | 12          | 12          | -           | 48    |
|              | $i_{\Sigma m+g}$ | 8           | 8           | 7           | 8           | -           | 31    |
|              | $c, c^*$         | 27          | 27          | 28          | 28          | -           | 110   |
| 0.1          | i                | 8           | 8           | 8           | 8           | -           | 32    |
|              | $i_{\Sigma m}$   | 4           | 3           | 5           | 7           | -           | 19    |
|              | $i_{\Sigma m+g}$ | 5           | 5           | 5           | 5           | -           | 20    |
|              | $c, c^*$         | 20          | 16          | 19          | 20          | -           | 75    |
| 0.07         | i                | 7           | 7           | 7           | 6           | -           | 27    |
|              | $i_{\Sigma m}$   | 2           | 2           | 2           | 2           | -           | 8     |
|              | $i_{\Sigma m+g}$ | 3           | 3           | 3           | 3           | -           | 12    |
|              | $c, c^*$         | 13          | 13          | 13          | 12          | -           | 51    |
| 0.04         | i                | 6           | 4           | 4           | 4           | -           | 18    |
|              | $i_{\Sigma m}$   | 1           | 0           | 0           | 2           | -           | 3     |
|              | $i_{\Sigma m+g}$ | 3           | 2           | 2           | 2           | -           | 9     |
|              | $c, c^*$         | 6           | 2           | 3           | 4           | -           | 15    |
| TOTAL        |                  | 1113        | 1092        | 1093        | 1099        | 497         | 4894  |

- means that cross section are being still determined.

## Theoretical simulation of the measured cross sections

Figs. 3-6 present experimental and simulated excitation functions for several products from  $^{208}\text{Pb}$  and  $^{\text{nat}}\text{Pb}$ . The simulations were made using the LAHET (ISABEL and BERTINI models), CEM03, INCL4+ABLA, CASCADE, LAQGSM+GEM2, YIELDX2000 codes. A short description of these codes can be found in [13] and references therein.

The predictive power of the tested codes is different but was found to be satisfactory for most of the nuclides in the spallation region, though none of the benchmarked codes agrees well with all the data in the whole mass region of product nuclides and all codes should be improved further.

## Acknowledgments

This work has been performed under the ISTC Project #2002 supported by the European Community and was partially supported by the U. S. Department of Energy and the NASA ATP01 Grant NRA-01-ATP-066.

## References

- [1] ISTC Project #2002, Proton-Pb and Proton-Bi Reaction Yields, <http://tech-db.istc.ru/istc/db/projects.nsf/all-projects/2002>.
- [2] Yu.E. Titarenko et al. Experimental and Theoretical Study of the Yields of Residual Product Nuclie in Thin Targets Irradiated by 100 – 2600 MeV Protons, IAEA, Nuclear Data Section, [INDC\(CCP\)-434](http://www-nds.iaea.org/reports/indc-ccp-434.pdf), September, 2002, <http://www-nds.iaea.org/reports/indc-ccp-434.pdf>.
- [3] Yu.E. Titarenko, O.V. Shvedov, V.F. Batyaev, et.al. Cross sections for nuclide production in 1 GeV proton-irradiated  $^{208}\text{Pb}$ . Phys.Rev., **C65** (2002) 064610.
- [4] Yu. E. Titarenko, O. V. Shvedov, M. M. Igumnov, et.al. Experimental and computer simulation study of the radionuclides produced in thin  $^{209}\text{Bi}$  targets by 130 MeV and 1.5 GeV proton induced reactions. Nucl. Instr. Meth., **A414**, 73-99 (1998).
- [5] M. Gloris, R. Michel, F. Sudbrok, et al., Proton-Induced Production of Residual Radionuclides In Lead at Intermediate Energies Nucl. Instr. and Meth., **A463**, 593 (2001); EXFOR file O0500.
- [6] Y. Y. Chu, G. Friedlander, L. Husain Production of Nuclides with Atomic Mass  $43 \leq A \leq 51$  In the Interaction of 1-28.5 GeV Protons with V, Ag, in, Pb and U Targets. Phys. Rev. C, v. 15, p. 352, 1977; EXFOR file O0399.
- [7] E. Hagebo, T. Lund. Fission of Lead Induced by 600 MeV Protons. J, JIN, v. 37, p. 1569, 1975; EXFOR file O0327 .
- [8] J. Hudis, S. Tanaka Production of Be-7, Na-22, And Na-24 Fragments From Heavy Elements at 3, 10, and 30 GeV. Phys. Rev., v. 171, p.1297, 1968; EXFOR file C0341 .
- [9] R.G. Korteling, A.A. Caretto. Systematics of Na-24 and Na-22 Production with 400 MeV Protons. J, JIN, v. 29, p. 2863, 1967; EXFOR file O0412.
- [10] J. A. Panontin, N. T. Porile., Recoil Properties and Charge Distribution in the Fission of Pb-208 by 450 MeV Protons. J, JIN, v. 30, p. 2891, 1968; EXFOR file O0332.
- [11] T. Enqvist, W. Wlazlo, P. Armbruster et al., Isotopic Yields and Kinetic Energies of Primary Residues in 1 A GeV  $^{208}\text{Pb} + \text{p}$  Reactions, Nucl. Phys. A686, 481 (2001); see also: Primary-Residue Production Cross Sections and Kinetic Energy in 1 A GeV  $^{208}\text{Pb}$  on Deuteron Reactions, Nucl. Phys. A703, 435 (2002). (0.5 GeV – private communication).
- [12] J. K. Tuli, Nuclear Wallet Cards, BNL, 6<sup>th</sup> edition, Jan. 2000.

- [13] Yu.E. Titarenko, V. F. Batyaev, V. M. Zhivun, et al., Theoretical Simulation of Residual Nuclide Products in  $^{208}$ ,  $^{207}$ ,  $^{206}$ Pb,  $^{nat}$ Pb And  $^{209}$ Bi (p,x) Reactions at Inter-Medium And High Energies. to be published in Proc. of ICRS-10/RPS 2004 Int. Conferences, Funchal, 10 May, 2004.
- [14] Yu.E. Titarenko, et al., Nuclide Production in  $^{197}$ Au ,  $^{208}$ Pb, and  $^{nat}$ U Irradiated with 0.8-1 GeV Protons: Comparison with other Experiments and with Theoretical Predictions, Workshop on Nuclear Data for the Transmutation of Nuclear Waste, GSI-Darmstadt, September 2003.

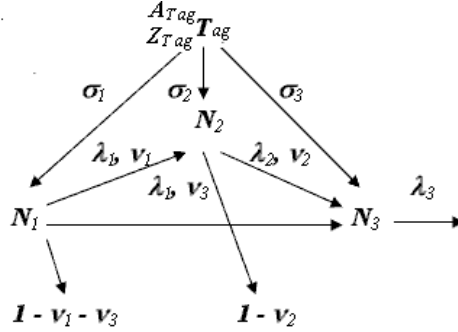


Fig. 2. Three chain decay scheme

$$\sigma_1^{cum} = \frac{1}{N_{Tag} \cdot \Phi} \cdot \frac{A_1}{F_1} \quad (1) \quad \sigma_1^{cum} = \frac{1}{N_{Tag} \cdot \Phi} \cdot \frac{B_1}{F_1} \cdot \frac{1}{\nu_{12}} \cdot \left( 1 - \frac{\lambda_1}{\lambda_2} \right) \quad (2)$$

$$\sigma_2^{ind} = \frac{1}{N_{Tag} \cdot \Phi} \cdot \left( \frac{B_2}{F_2} + \frac{B_1}{F_1} \cdot \frac{\lambda_1}{\lambda_2} \right) \quad (3) \quad \sigma_2^{cum} = \sigma_2^{ind} + \nu_{12} \cdot \sigma_1^{cum} = \frac{1}{N_{Tag} \cdot \Phi} \left( \frac{B_1}{F_1} + \frac{B_2}{F_2} + \frac{B_1}{F_1} \cdot \frac{\lambda_1}{\lambda_2} \right) \quad (4)$$

$$\sigma_1^{cum} = \frac{1}{N_{Tag} \cdot \Phi} \cdot \frac{C_1}{F_1} \cdot \frac{1}{\nu_{13} + \nu_{12} \cdot \nu_{23} \cdot \frac{\lambda_2}{\lambda_2 - \lambda_1}} \cdot \left( 1 - \frac{\lambda_1}{\lambda_3} \right) \quad (5)$$

$$\sigma_2^{ind} = \frac{1}{N_{Tag} \cdot \Phi} \left[ \frac{C_2}{F_2} \cdot \frac{1}{\nu_{23}} \cdot \left( 1 - \frac{\lambda_2}{\lambda_3} \right) + \frac{C_1}{F_1} \cdot \nu_{12} \cdot \frac{\frac{\lambda_1}{\lambda_2 - \lambda_1}}{\frac{\lambda_2}{\lambda_2 - \lambda_1} \cdot \left( \nu_{13} + \nu_{12} \cdot \nu_{23} \cdot \frac{\lambda_2}{\lambda_2 - \lambda_1} \right)} \right] \quad (6)$$

$$\sigma_2^{cum} = \sigma_2^{ind} + \nu_{12} \cdot \sigma_1^{cum} = \frac{1}{N_{Tag} \cdot \Phi} \left[ \frac{C_2}{F_2} \cdot \frac{1}{\nu_{23}} \cdot \left( 1 - \frac{\lambda_2}{\lambda_3} \right) + \frac{C_1}{F_1} \cdot \nu_{12} \cdot \frac{\frac{\lambda_1}{\lambda_2 - \lambda_1}}{\frac{\lambda_2}{\lambda_2 - \lambda_1} \cdot \left( \nu_{13} + \nu_{12} \cdot \nu_{23} \cdot \frac{\lambda_2}{\lambda_2 - \lambda_1} \right)} \right] \quad (7)$$

$$\sigma_3^{ind} = \frac{1}{N_{Tag} \cdot \Phi} \cdot \left[ \frac{C_3}{F_3} + \frac{C_2}{F_2} \cdot \frac{\lambda_2}{\lambda_3} + \frac{C_1}{F_1} \cdot \frac{\lambda_1}{\lambda_3} \right] \quad (8)$$

$$\sigma_3^{cum} = \sigma_3^{ind} + \nu_{13} \cdot \sigma_1^{cum} + \nu_{23} \cdot \sigma_2^{cum} + \nu_{12} \cdot \nu_{23} \cdot \sigma_1^{cum} = \frac{1}{N_{Tag} \cdot \Phi} \cdot \left[ \frac{C_1}{F_1} + \frac{C_2}{F_2} + \frac{C_3}{F_3} \right] \quad (9)$$

where  $\sigma_1^{cum}, \sigma_2^{ind}, \sigma_2^{cum}, \sigma_3^{ind}, \sigma_3^{cum}$  - independent and cumulative cross sections,  $N_1, N_2, N_3; N_{Tag}$  - number of nuclei of  $^{A_{Tag}}Z_{Tag}T_{ag}$  in experimental target;  $\Phi$  - average flux of protons;  $A_1, B_1, B_2, C_1, C_2, C_3$  - factors defined by experimental points fitting;  $F_1, F_2, F_3$  - saturation functions;  $\nu_{12}, \nu_{13}, \nu_{23}$  - branching factors;  $\lambda_1, \lambda_2, \lambda_3$  - decay constants.

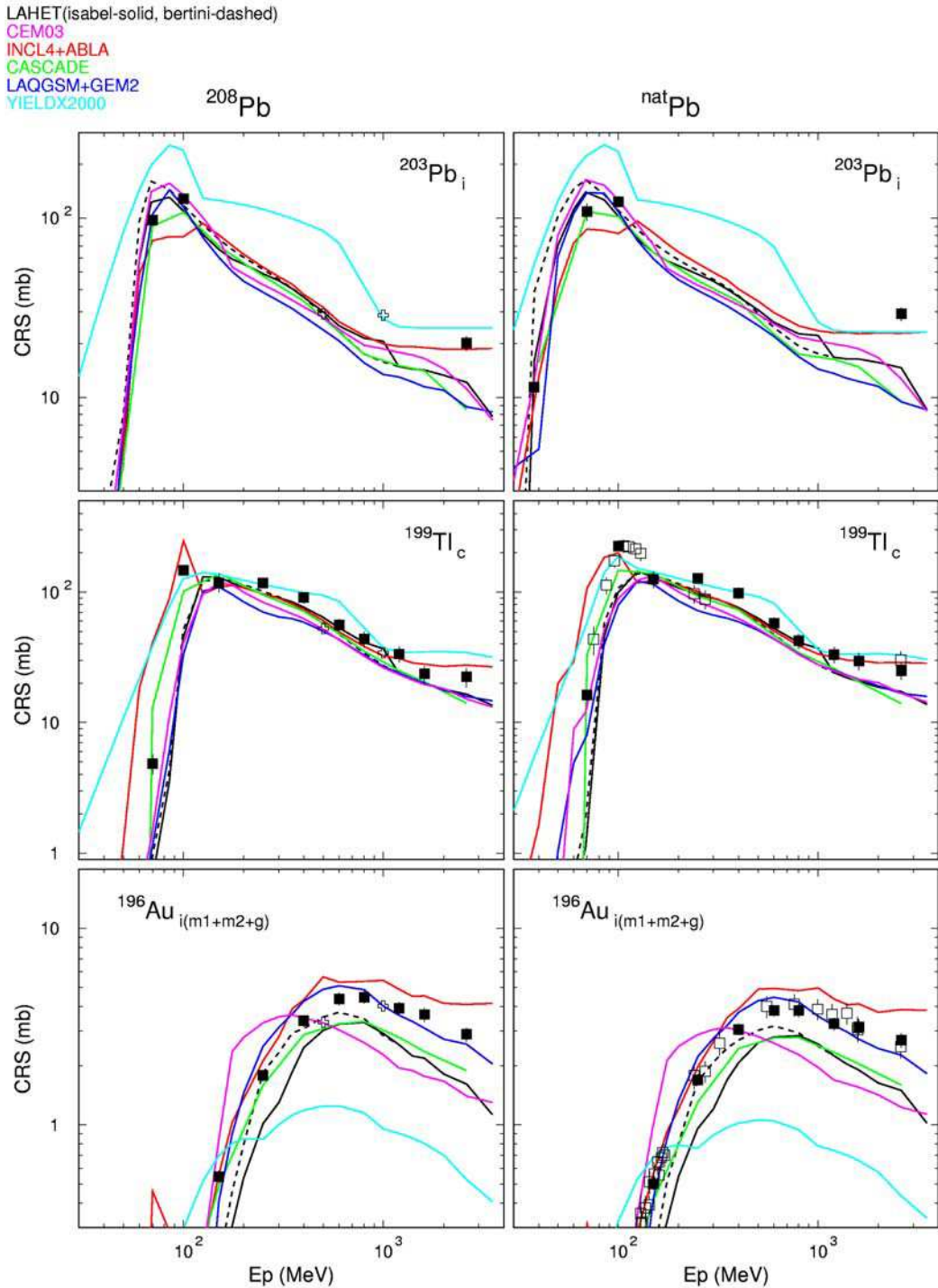


Fig. 3. Experimental and simulated excitation functions of  $^{203}\text{Pb}$ ,  $^{199}\text{Tl}$ ,  $^{196}\text{Au}$  produced in  $^{208}\text{Pb}$  (left) and  $^{nat}\text{Pb}$  (right). (■ – this work; □ – [5]; Δ – [7]; ∆ – work [8], ▽ – [11]) ( LAHET –black (ISABEL - solid, BERTINI – dashed), CEM03 - magenta, INCL4+ABLA – red, CASCADE – green, LAQGSM+GEM2 – blue, YIELDX2000 – green-blue).

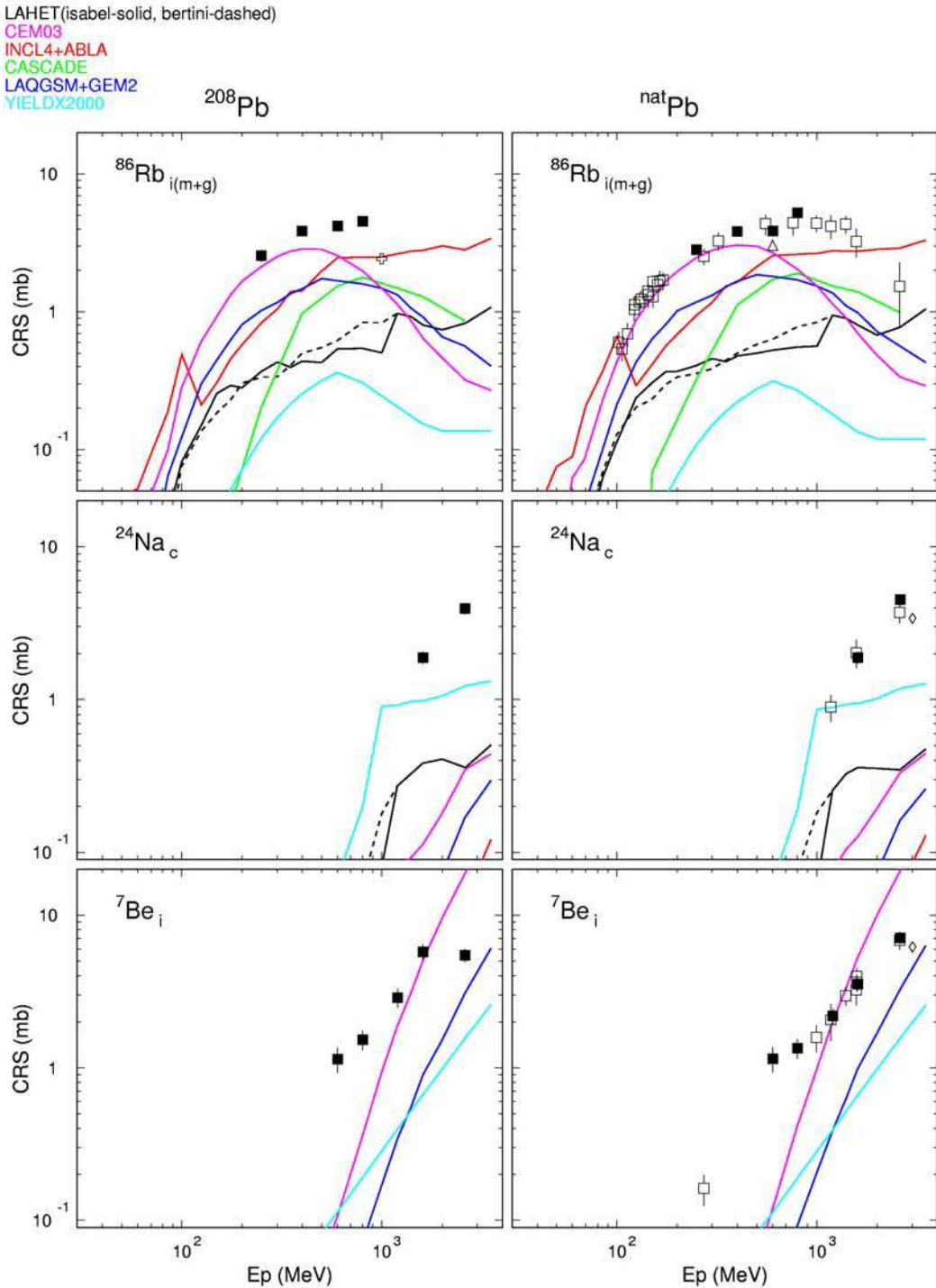


Fig. 4. Experimental and simulated excitation functions of  $^{86}\text{Rb}$ ,  $^{24}\text{Na}$ ,  $^7\text{Be}$  produced in  $^{208}\text{Pb}$  (left) and  $^{\text{nat}}\text{Pb}$  (right). (■ – this work; □ – [5]; Δ – [7]; ◇ – [8], ▨ – [11]) ( LAHET –black (ISABEL - solid, BERTINI – dashed), CEM03 - magenta, INCL4+ABLA – red, CASCADE – green, LAQGSM+GEM2 – blue, YIELDX2000 – green-blue)

LAHET(isabel-solid, bertini-dashed)

CEM03

INCL4+ABLA

CASCADE

LAQGSM+GEM2

YIELDX2000

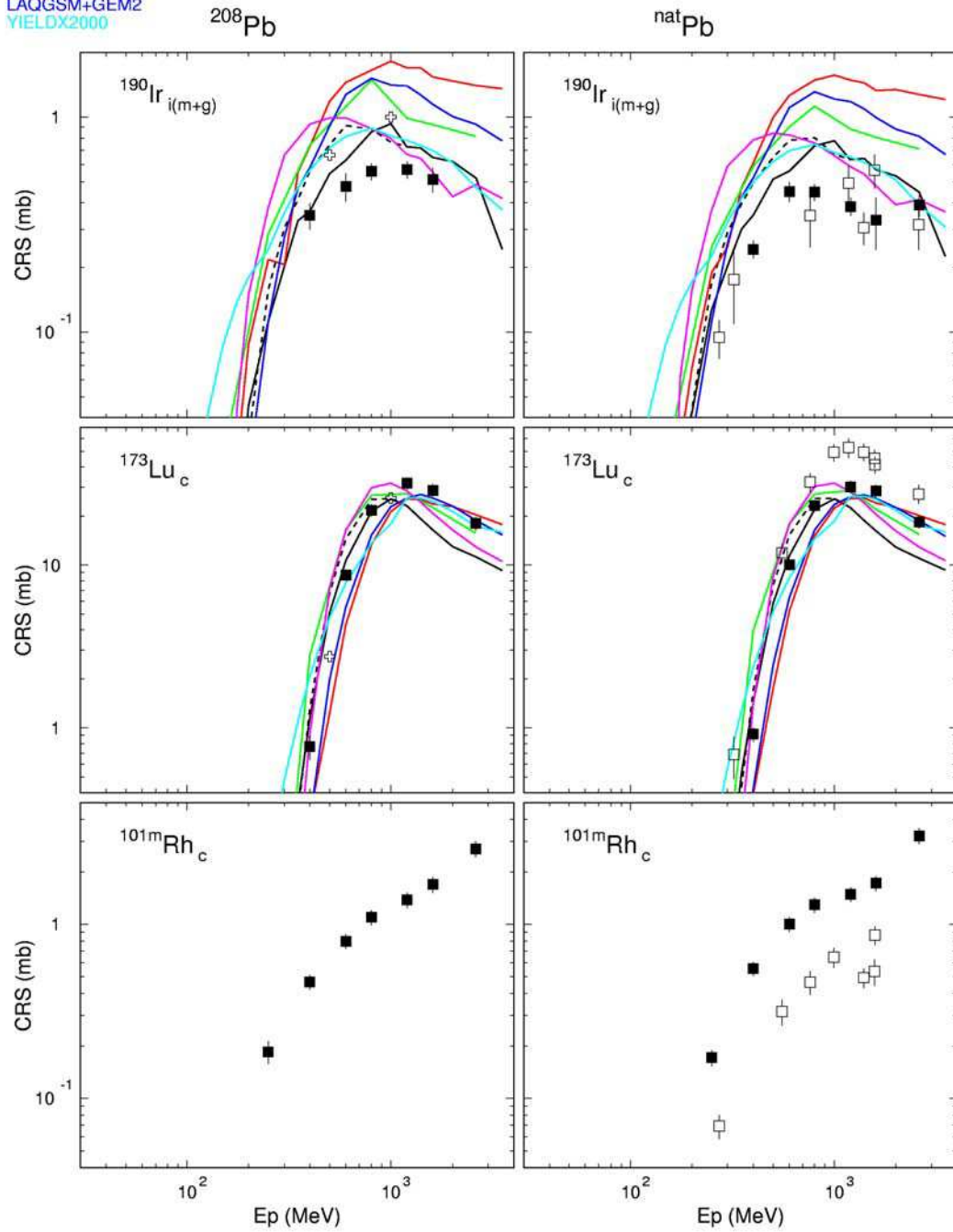


Fig. 5. Experimental and simulated excitation functions of  $^{190}\text{Ir}$ ,  $^{173}\text{Lu}$ ,  $^{101\text{m}}\text{Rh}$  produced in  $^{208}\text{Pb}$  (left) and  $^{\text{nat}}\text{Pb}$  (right). (■ – this work; □ – [5]; Δ – [7]; ◇ – [8],  $\frac{1}{2}$  – [11]) ( LAHET –black (ISABEL - solid, BERTINI – dashed), CEM03 - magenta, INCL4+ABLA – red, CASCADE – green, LAQGSM+GEM2 – blue, YIELDX2000 – green-blue).

LAHET(isabel-solid, bertini-dashed)

CEM03

INCL4+ABLA

CASCADE

LAQGSM+GEM2

YIELDX2000

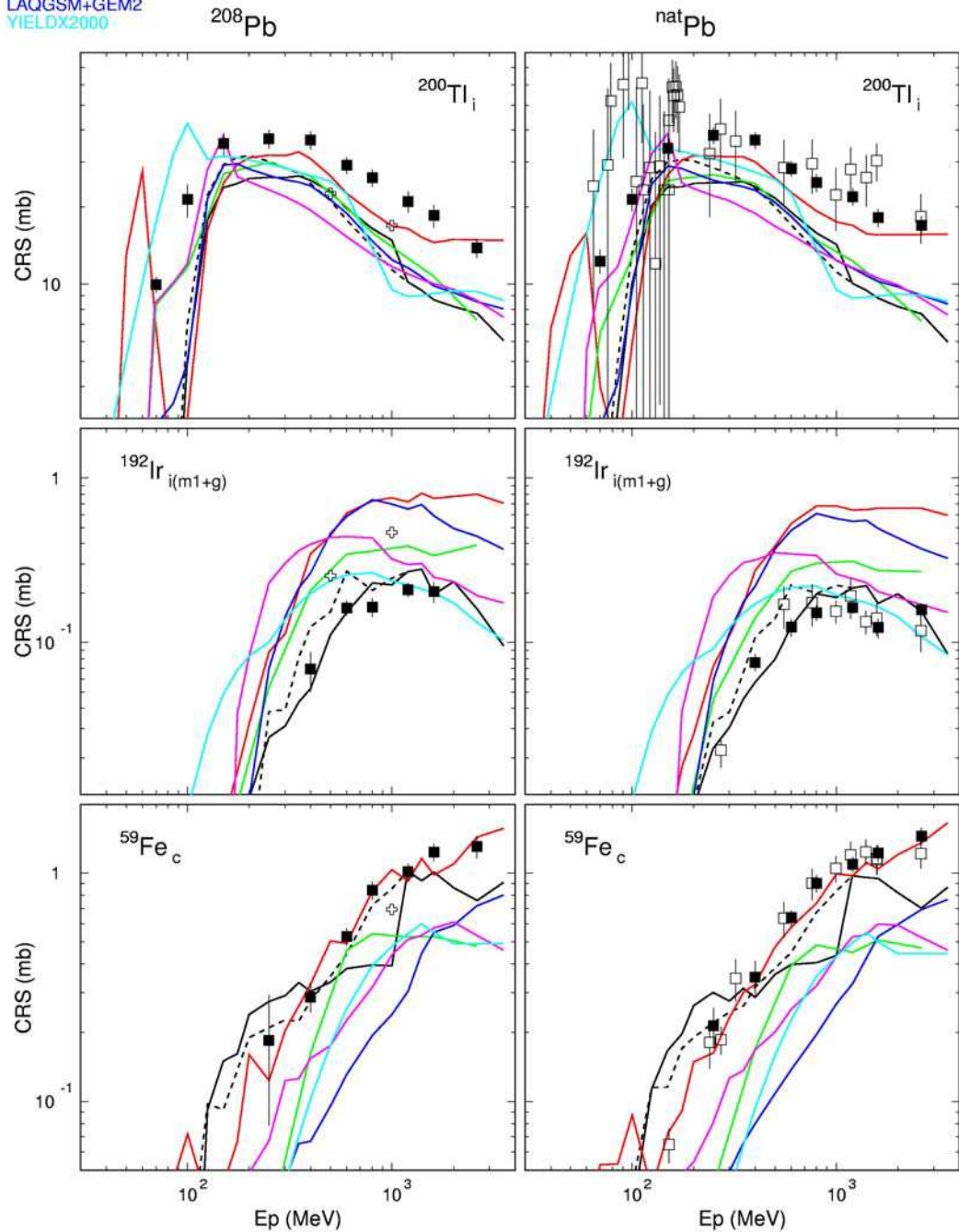


Fig. 6. Experimental and simulated excitation functions  $^{200}\text{Tl}$ ,  $^{192}\text{Ir}$ ,  $^{59}\text{Fe}$ , produced in  $^{208}\text{Pb}$  (left) and  $^{\text{nat}}\text{Pb}$  (right). (■ – this work; □ – [5]; Δ – [7]; ◇ – [8], ▨ – [11]) ( LAHET –black (ISABEL - solid, BERTINI – dashed), CEM03 - magenta, INCL4+ABLA – red, CASCADE – green, LAQGSM+GEM2 – blue, YIELDX2000 – green-blue).